

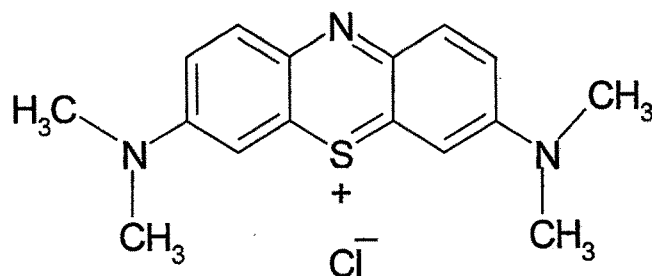
## **CHAPTER 2**

# **ADSORPTION STUDIES OF CATIONIC DYES WITH PALM SHELL POWDER**

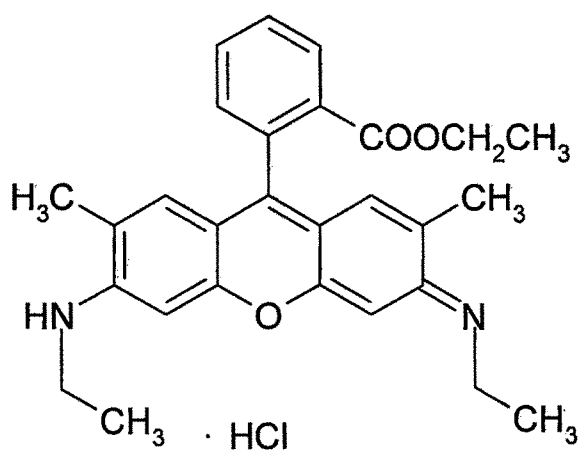
## 2.1 Introduction

During textile processing, inefficiencies in dyeing result in a large amount of dyestuff being directly lost in the wastewater, which ultimately finds way into the environment. It is estimated that 5–10% of the dyes is lost in the effluent during the dyeing process. Dyes can be classified as follows [2.1]: anionic (direct, acid and reactive dyes), cationic (basic dyes) and non-ionic (dispersive dyes). Basic dyes, which are predominantly used in colouring acrylic fibre, are generally more toxic than other classes of dyes [2.2]. Methylene blue is a cationic dye of thiazine class which is most commonly used for colouring paper, temporary hair colorant, dyeing cottons, wools, etc. Though Methylene blue is not strongly hazardous it can cause some harmful effects. Acute exposure to Methylene blue will cause increased heart rate, vomiting, shock, Heinz body formation, cyanosis, jaundice, quadriplegia and tissue necrosis in humans [2.3]. Methylene Blue can cause eye burns which may be responsible for permanent injury to the eyes of humans and animals [2.4]. Rhodamine B (RhB) is a highly water soluble, basic red dye of the xanthene class. It is a typical cationic dye that has been widely used as a colorant in textiles and food stuffs. It is also a well-known fluorescent water tracer and biological stains. Thus, the study of removal of basic dyes, with Methylene Blue (MB) and Rhodamine 6G as model dyes from the environmental is worthwhile. The objective of the study was to investigate the potential of palm shell powder (PSP) (*Borassus flabellifer*) for the removal of these dyes from aqueous solutions. Column adsorption, equilibrium, adsorption kinetics, effect of dose and effect of pH were studied and the efficacy of the adsorbent was compared with commercially activated carbon in granular form (CAC).

Structures of Cationic Dyes



Methylene Blue



Rhodamine 6G

2.2 Processing of Palm shell Powder:

Palm shells, the agricultural wastes of palm fruits, which are available abundantly in coastal Andhra Pradesh, were used in the present study. The scientific name of this palm is *Borassus flabellifer*. The shells were washed to remove mud and sun dried for 24 hrs and then crushed by using jaw crusher. Powder of 70 microns size was separated and again washed thoroughly with distilled water and kept in water for 48 hours by changing water for every 10 hrs and then removed and washed finally and dried for 4 hrs at 110°C. The processed powder was characterized and used in further experiments. The prepared palm shell powder from herewith is referred to as PSP.

### **2.3 Characterization of the PSP:**

The prepared PSP has been characterised for physical properties (bulk density, moisture content, solubility in water and acid) and chemical properties (pH, ion exchange capacity, iodine number). Spectral analysis of the samples using FTIR is also done. Thermal analysis using TG/DTA, Surface area analysis with BET, topographic analysis using SEM and X-ray studies were also done.

#### **2.3.1 Bulk density:**

For measuring the bulk density of the material a 100mL graduated cylinder was weighed accurately and filled to 50mL mark with carbon. The cylinder with the carbon was weighed accurately. The apparent density was calculated by dividing the difference in weight by 50 (Table 2.1).

#### **2.3.2 Solubility in water:**

Determination of solubility in water was done by taking ten gram of carbon into a one litre beaker and boiled with 300mL distilled water and 0.25N HCl respectively followed by digestion for around 30min. The material was washed thoroughly with distilled water and washings were collected along with the filtrate. The filtrate was concentrated on a water bath, cooled and made up to 100mL in a volumetric flask. Exactly 50mL of the concentrate was transferred to a china dish, evaporated to almost dryness on a water bath and finally dried in an electric oven maintained at  $105 \pm 5^{\circ}\text{C}$ , cooled and weighed. The weight of the residue represents the matter soluble in water and acid (Table 2.1).

### 2.3.3 pH of adsorbent:

The pH was measured by heating a suspension of ten gram carbon in 300mL distilled water to boiling with constant stirring. The solution was then digested for around 30 minutes. The material was filtered, cooled and pH of the solution was measured (Table 2.1).

### 2.3.4 Ion Exchange Capacity:

For measuring the Ion Exchange capacity, 0.5 g carbon was added to 100 mL solution of 0.25M sodium sulphate in a stoppered conical flask and kept for shaking in a temperature controlled shaking bath for 5 hours. The contents were filtered and the filtrate was titrated against 0.1N NaOH using phenolphthalein indicator. The ion exchange capacity of the carbon in meq/g (Table 2.1) was calculated from the following equation.

$$\text{Ion exchange capacity (meq/g)} = aW/V$$

Where, a = Normality of NaOH, V =Volume of NaOH, W =Weight of the carbon in g

**Table 2.1: Physical properties of Palm Shell Powder**

Physical property	Value
Bulk density g/cc	0.27
pH	6.4
Ion-exchange capacity meq/g	0.05
Matter soluble in water (%)	0.84
Carbon (%)	45.14
Hydrogen (%)	5.59
Nitrogen (%)	0.73

### 2.3.5 Surface Area Analysis:

Adsorption characteristics of the PSP samples were determined by nitrogen adsorption at 77.37K (Surface Area Analyser Micromeritics, ASAP 2020 V3.03H). The specific surface area as determined from the isotherms using the Brunauer–Emmett–Teller equation. The pore volume and the BJH method was used for pore size distribution determination [2.5, 2.6] (Table 2.1).

**Table 2.2: Surface area analysis data of PSP**

Adsorbent	Single point SA	BET SA	Langmuir SA	BJH Pore Volume	BET Av. Pore dia.
Unit	m <sup>2</sup> /g	m <sup>2</sup> /g	M <sup>2</sup> /g	cm <sup>3</sup> /g	Å
PSP	0.5623	0.6735	0.9659	0.00401	237.984

### 2.3.6 Scanning Electron Micrograph (SEM):

Scanning Electron Microscope (SEM) is an instrument that uses a beam of highly energetic electrons to examine objects on a very fine scale. The shape, size and arrangement of the particles making up the object that are lying on the surface of the sample or have been exposed by grinding or chemical etching; detectable features limited to a few manometers. Scanning electron micrograph (SEM) was recorded at 1×1500 magnification using a Scanning electron microscope JSM -5610LV model with energy dispersive analytical X-ray (EDAX). The SEM clearly reveals the surface texture and porosity of adsorbent with holes as displayed in Figure 2.1. The small openings found on the surface indicate that it would increase the contact area and facilitate pore diffusion during adsorption.

### **2.3.7 X-ray diffraction studies:**

X-ray powder diffraction is a standard tool for the identification of amorphous solid phases. In a real crystal the lattice points are occupied by atoms and hence, the crystal lattice acts as a three dimensional diffraction grating for x-rays as they have wavelength of the dimensions of interatomic distances in a crystal. Powder diffractograms are obtained by measuring the angles at which an x-ray beam of wavelength  $\lambda$  is diffracted by the sample. Position, intensity, shape and width of the diffraction line give information about the spacing between two planes (hkl). The distance between two successive parallel planes in the crystal (d) is related to the diffraction angle  $2\theta$  by Bragg's law.

$$\lambda = 2d \sin\theta$$

Powder-XRD of the ingredients was taken by holding the sample in place on quartz plate for exposure to  $\text{CuK}\alpha$  radiation of wavelength 1.5406 Å. The sample was analyzed at room temperature over a range of  $10\text{-}70^\circ 2\theta$  with sampling intervals of  $0.02^\circ 2\theta$  and scanning rate of  $6^\circ/\text{min}$ .

The study reveals that the adsorbent is crystalline and amorphous in nature as shown in Figure 2.2

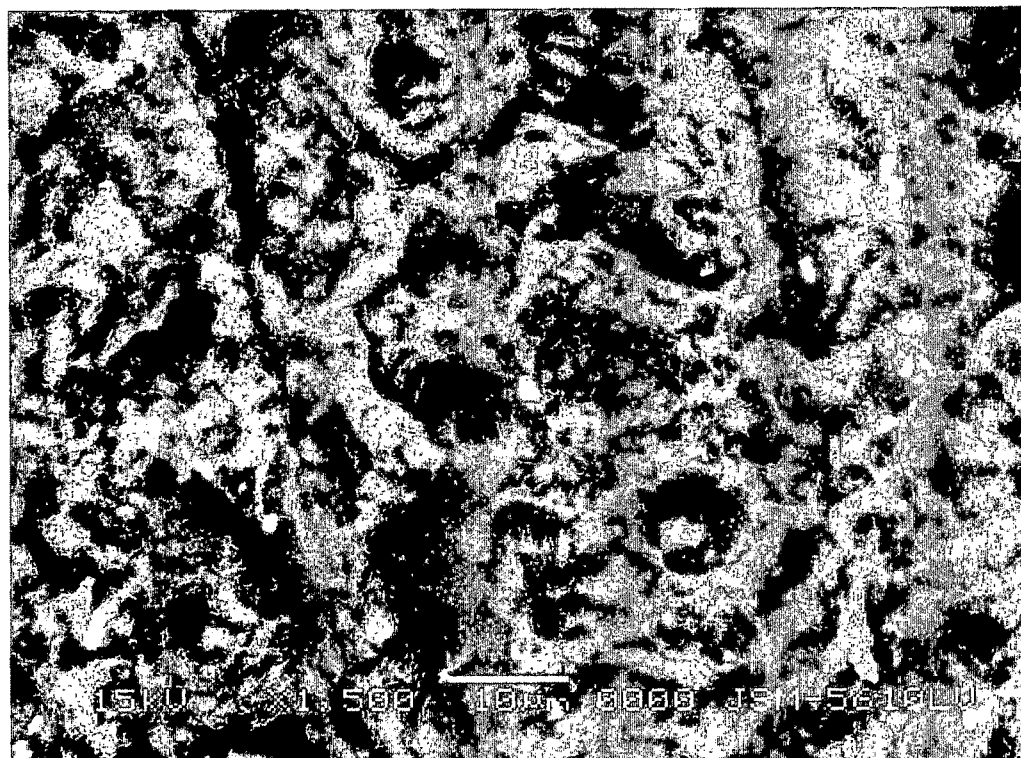


Figure 2.1: Scanning Electron Micrograph of PSP at 1,500 magnifications

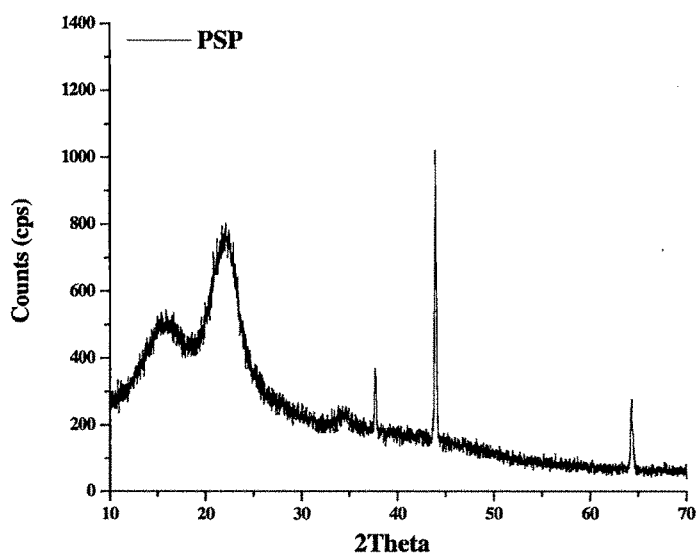


Figure 2.2: XRD graph of PSP

### **2.3.8 Infrared Spectroscopy:**

Infrared spectroscopy is based upon the interaction of electromagnetic radiation with matter. Every solid, liquid or gaseous material is built up of aggregates of molecules or periodic lattice of well defined molecules or atoms. Majority of such systems of matter exhibit local dipole moment depending upon mass, binding force, distances and relative angle of atoms, which make up molecules or system of molecules. Each of these has a set of characteristic vibrational states, which are typical of a material. The various properties of a material are dependent upon its microstructure, which can be understood from the IR spectra of the material. Vibrational spectroscopy is the most promising and widely used method for characterization of materials. The advantage being that detailed micro structural information is obtained from the vibrational spectra. The information obtained from IR spectra serves as both complementary and supplementary to those obtained from other techniques like XRD. In the present study the spectra were collected by a Perkin Elmer RX1 model within the wave number range of 400-4000 $\text{cm}^{-1}$ . Specimens of samples were first mixed with KBr and then ground in an agate mortar at an appropriate ratio of 1/100 for the preparation of the pellets.

Resulting mixture was pressed at 10 tons for 5 min. sixteen scans and 8 $\text{cm}^{-1}$  resolution were applied in recording spectra. The background obtained from the scan of pure KBr was automatically subtracted from the sample spectra.

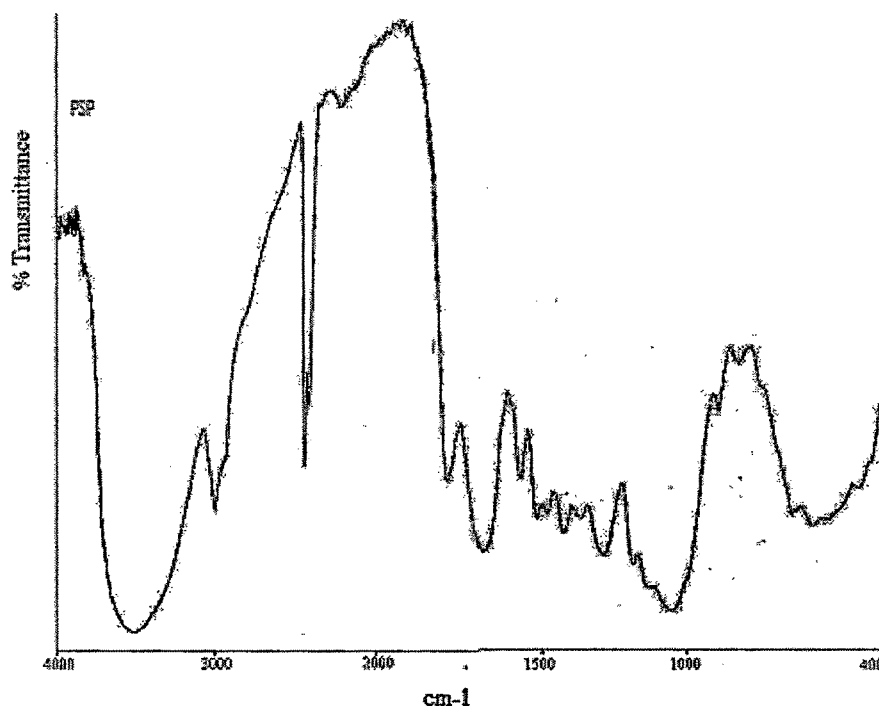


Figure 2.3: FTIR Spectrum graph of PSP

Table 2.3: IR Data of PSP

Sample	PSP	Intensity	Assignment
Wave numbers (cm <sup>-1</sup> )	3422.37	Strong	N-H & OH Stretching
	1739.43	Strong	Lactones & 5-membered rings
	1622.64, 1510.19,	Variable	
	1460.53	Variable	C=O, N-H bending
	1379.06, 1250.52		C-O, C-H bending

#### 2.4 Preparations of the solutions:

All the chemicals used were of highly pure and commercially available AnalaR grade of Sulab Chemicals, Vadodara (India).

#### **2.4.1 Cationic dye Solution:**

Stock solutions of dyes (1g/L) were prepared by dissolving accurately weighed amount of individual dye in double distilled water and subsequently diluted to the required concentration.

#### **2.5 Batch adsorption studies of Cationic dyes:**

Adsorption studies were carried out with 100mL Durasil Stopped flasks in a thermo regulated water bath at 25°C. A 25 mL of dye solution of known initial concentration was kept in contact with a required dose of PSP at constant agitation at 200rpm. The pH of solution was adjusted using 0.1M HCL and 0.1M NaOH using pH meter (MFRS: TOSHNIWAL INST. MFG. PVT. LTD. AJMER, CAT. NO. CL54). After a specific stirring time period the reaction mixture was filtered using whatmann filter paper and the filtrate was analysed to determine the residual adsorbate concentration. The dye concentration in the filtrate was determined by measuring the absorbance at the wavelength of maximum absorption (609 nm for MB and 524 nm for Rh6G) using a SYSTRONICS Digital 166 model visible spectrophotometer. The concentrations were determined from their respective calibration graphs (Figure 2.4). The percentage removal of the dye and the amount adsorbed (mg/g) were calculated by the following relationship:  $100(C_i - C_f) / C_i$  where  $C_i$  is the initial concentration of the dye (mg/L) and  $C_f$  is the concentration of the dye present in solution after adsorption for a particular time interval (mg/L).

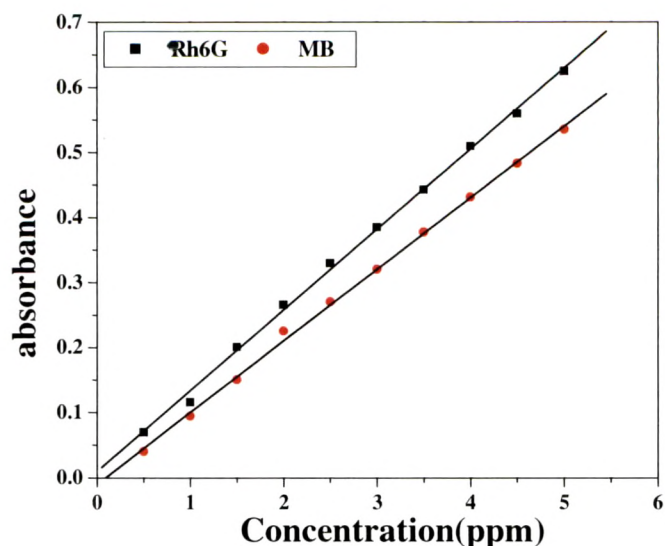


Figure 2.4: Calibration graph of Rh 6G and MB

## 2.6 Optimization parameters for adsorption of Cationic Dyes:

### 2.6.1 Effect of pH on adsorption of cationic dyes:

pH plays a very important role in effective decolourisation of dye colour of any adsorbate-adsorbent system. pH of the system affects the nature of the surface charge of the adsorbent, ionization of dye and the extent and rate of adsorption. The hydrogen ion concentration (pH) primarily affects the degree of ionization of the dyes and the surface properties of PSP. These, in turn, lead to alterations in the amount of adsorbate removed. The effect of pH on the adsorption behaviour of cationic dyes on PSP was investigated by the batch process in the pH range 2-10 using 100 ppm of dyes (Rhodamine 6G, Methylene blue). The pH was adjusted to the desired value and the volume was maintained at 25mL. After addition of 0.1g of PSP and CAC the solutions were agitated for 2 hours. The solutions were filtered and analysed by the methods described in analyses of each adsorbate. With PSP as adsorbent, the

maximum adsorption of the dyes was observed above pH 4.0 in the case of Methylene blue. From Figure 2.5 and Table 2.4 it was observed that there was no significant variation in adsorption capacity with change in pH above 4.0. This could be probably due to the fact that at high pH, OH<sup>-</sup> on the surface of adsorbent will favour the adsorption of cationic dye molecule. In the case of Rh6G also it was observed that adsorption is optimum in the alkaline range and there was only 2% variation in percentage adsorption between pH 6 and pH 10. Hence the rest of the parameters were optimized at the original pH of the respective dye solutions itself. The pH of Rh6G solution is 5.75 and that of MB solution is 6.54.

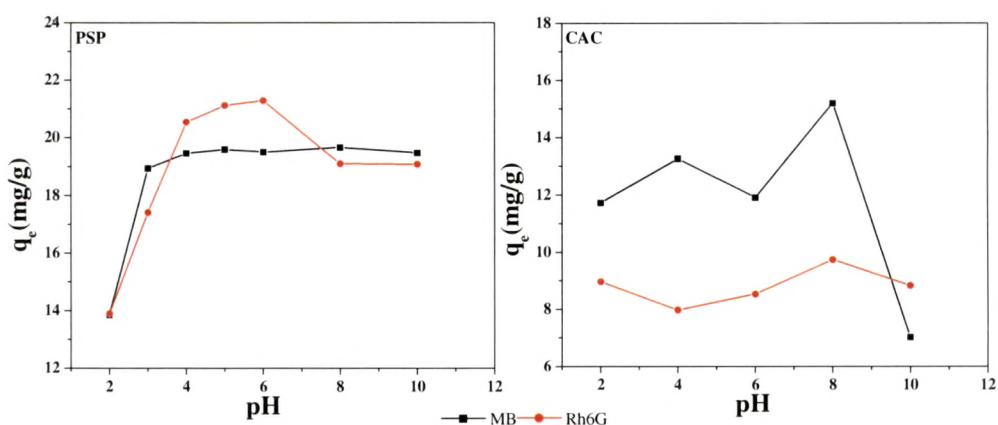


Figure 2.5: Effect of pH on the adsorption of MB and Rh6G on PSP and CAC

**Table 2.4: Percentage uptake of cationic dyes at different pHs on PSP and CAC**

Adsorbent: PSP, CAC; adsorbate: Rhodamine 6G, Methylene blue; Temperature: 30°C, Initial concentration: 100ppm, Wt. of adsorbent: 0.1g; Volume of aqueous phase: 25mL, Contact time: 120min. pH: 1-9.

pH	Percentage uptake of cationic dyes			
	PSP		CAC	
	MB	Rh6G	MB	Rh6G
2	67.3664	55.1232	48.95	35.7966
3	94.75	80.1642	-	-
4	97.0176	91.95	54.8969	36.3101
5	97.4847	92.378	-	-
6	97.4295	92.873	56.98	37.6425
7	97.64	93.7708	-	-
8	97.839	94.4576	61.81	42.8148
10	98.45	95.2978	62.686	44.16

### 2.6.2 Effect of agitation time and dose on adsorption of cationic dyes:

The optimum dose for the maximum adsorption of respective adsorbate species under study was established from 25mL of aqueous phase onto 0.05 to 0.4 g of PSP and 0.2 to 1.0 g of CAC. The concentration of adsorbate used was 100ppm (Methylene Blue and Rhodamine 6G) in case of PSP and CAC as adsorbent. The effect of agitation time was investigated by varying the agitation time between 10 to 120 minutes. The percentage adsorbed in each instance was established and the results are tabulated in Table 2.5 and 2.6.

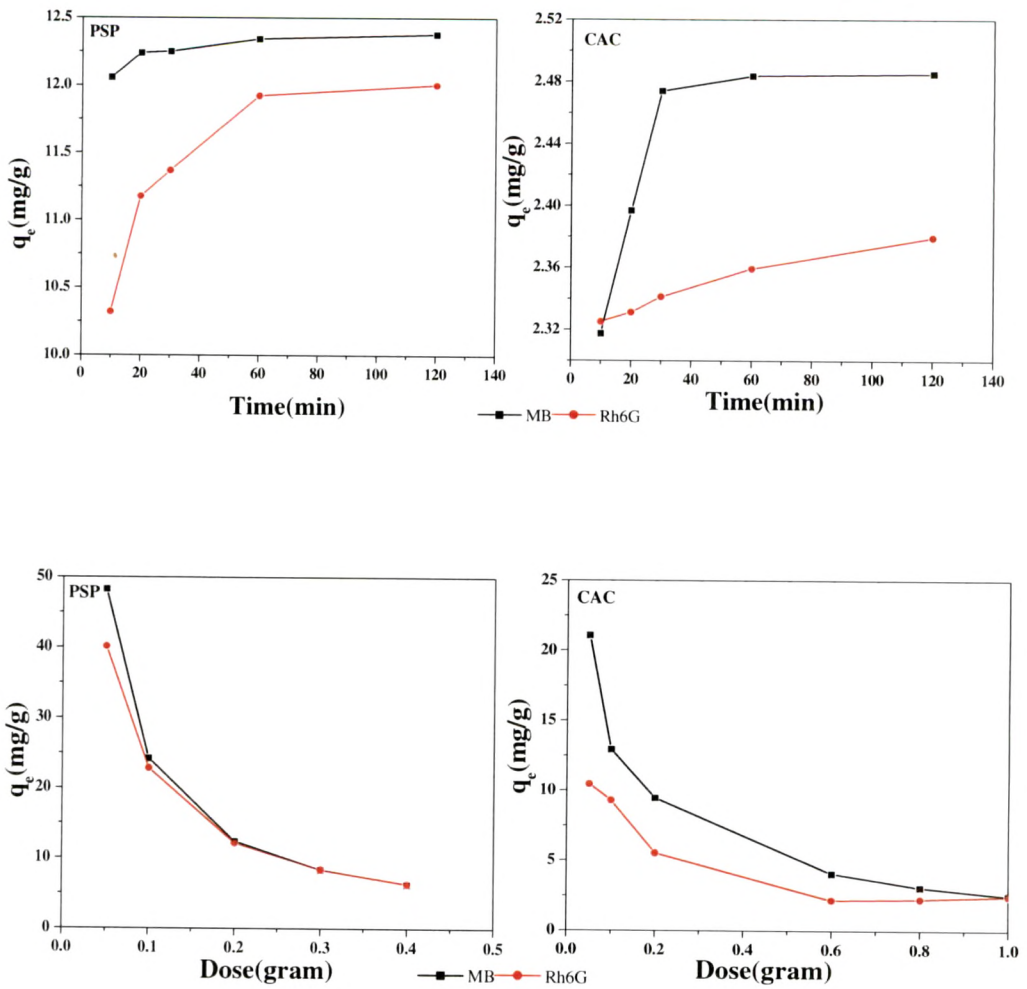


Figure 2.6: Effect of dose and time on the adsorption of MB and Rh6G

**Table 2.5: Effect of adsorbent dose and Variation of time on MB & Rh6G by PSP**

Adsorbent: PSP; adsorbate: Rhodamine 6G, Methylene blue; Temperature: 30°C, Initial concentration: 100ppm, Wt. of adsorbent: (0.05-0.4) g; Volume of aqueous phase: 25mL, Contact time: (10-120) min, pH: 6.54(MB), 5.75(Rh6G)

Dose (g)	Percentage uptake of Cationic dyes									
	0.05		0.1		0.2		0.3		0.4	
	M.B	Rh 6G	M.B	Rh 6G	M.B	Rh 6G	M.B	Rh 6G	M.B	Rh 6G
10	73.88	59.84	85.35	72.11	96.90	82.50	98.85	94.24	99.02	98.49
20	80.69	61.41	89.92	74.29	98.00	89.25	98.96	97.164	99.10	98.7
30	92.16	62.26	93.38	75.00	98.60	91.00	99.01	97.64	99.34	98.73
60	92.63	73.52	95.52	85.54	98.90	95.25	99.05	98.27	99.37	98.82
120	96.55	80.47	96.83	90.94	99.19	95.75	99.36	98.88	99.48	99.08

The effect of varying the PSP and CAC mass on aqueous dye solution are presented in Table 2.5 and 2.6. Of the two adsorbents, PSP gave the greater removal at all levels of the adsorbent dose. From Figure 2.6 it is seen that as the dose of the adsorbent increased with respect to the agitation time the  $q_e$  value was decreased in the case of both the dyes on the adsorption of PSP and CAC respectively.

**Table 2.6: Effect of adsorbent dose and variation of time on MB & Rh6G by**

**CAC**

Adsorbent: CAC, adsorbate: Rhodamine 6G, Methylene blue; Temperature: 30°C, Initial concentration: 100ppm, Wt. of adsorbent: (0.2-1.0) g; Volume of aqueous phase: 25mL, Contact time: (10-120) min, pH: 6.54(MB), 5.75(Rh6G)

Dose(g)	Percentage uptake of Cationic dyes							
	0.2		0.6		0.8		1.0	
	M.B	Rh 6G	M.B	Rh 6G	M.B	Rh 6G	M.B	Rh 6G
10	30.5	25.00	65.018	25.78	82.276	41.015	93.47	93.125
20	39.88	26.172	68.75	26.56	90.205	44.53	96.735	93.35
30	46.36	26.95	78.54	32.03	93.47	48.046	99.029	93.75
60	49.16	34.375	87.406	41.406	98.787	51.56	99.43	94.453
120	79.94	41.796	97.49	48.437	98.805	67.187	99.496	95.23

Initially the rate of increase in the percent dye removal has been found to be rapid which slowed down as the dose increased. With rise in adsorbent dose, there is less commensurate increase in adsorption, resulting from lower adsorptive capacity utilization of adsorbent [2.8]. The rate of adsorption is higher in the beginning as sites are available and unimolecular layer increases. The subsequent slow rise observed in percent removal suggests that adsorption and intra-particle diffusion could be taking place simultaneously with dominance of adsorption. Thus, the results obtained indicate that PSP has a large potential as an adsorbent for dye removal than CAC.

### 2.6.3 Effect of concentration on the adsorption of cationic dyes:

The effects of initial concentration of MB or Rh6G on the amount of dye adsorbed on PSP were studied to obtain the adsorption capacity. Different concentrations of the respective dyes (Methylene Blue and Rhodamine 6G) ranging from 100–500 ppm in a total aqueous phase volume of 25 mL, with the pH of the medium maintained at 6.54 for MB and 5.75 for Rh 6G was agitated with 1.0g of PSP for two hours and the amounts adsorbed on respective adsorbent were determined as described earlier. It was observed that adsorption of dye decreased with an increase in dye concentration in the solution, suggesting that removal of dye is dependent upon the concentration of the dye solution. But as a whole the  $q_e$  value increased with the increase in dye concentration as observed in the plot in Figure 2.7. From Table 2.7 it was observed that as the concentration of dye increased the percentage removal decreased indicating that the number of adsorption sites on the adsorbent decreases by increasing adsorbate concentration.

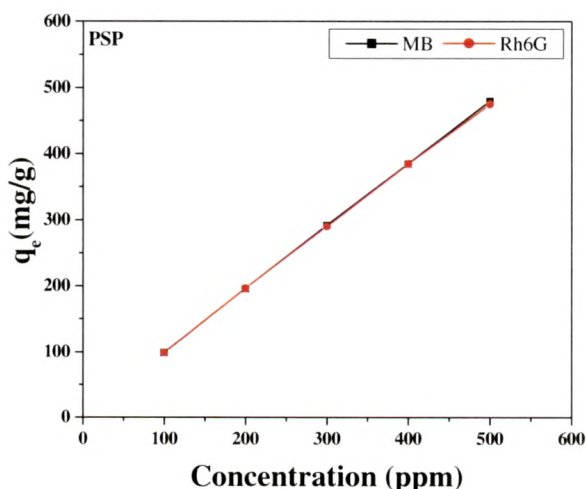


Figure 2.7: Effect of concentration of MB and Rh6G adsorption on PSP

**Table 2.7: Effect of variation in concentration of MB and Rh6G**

Adsorbent: PSP; adsorbate: Rhodamine 6G, Methylene blue; Temperature: 30°C, Initial concentration: (100-500) ppm, Wt. of adsorbent: 1.0 g; Volume of aqueous phase: 25mL, Contact time: 120 min. pH: 6.54(MB), 5.75(Rh6G)

Concentration (ppm)	Percentage uptake of Cationic dyes	
	MB	Rh6G
100	98.93	98.61
200	97.84	97.88
300	97.31	96.63
400	96.23	96.09
500	95.96	94.98

#### 2.6.4 Effect of temperature on the adsorption of dyes:

Effect of temperature on the adsorption kinetics of PSP and CAC were conducted at a pH of 6.54 for MB, 5.75 for Rh6G and 100 mg L<sup>-1</sup> initial dye concentration. From Figure 2.8 it can be seen that as the temperature increases from 40 to 70°C the corresponding  $q_e$  values increase suggesting physisorption as the mechanism in the case of PSP while the reverse order of  $q_e$  in the case of CAC indicates the chemisorption to be the mechanism as the temperature increases from 30 to 70°C.

From Table 2.8 and 2.9 it is seen that with increasing temperature from 40 to 70°C the adsorption capacity of PSP decreased. This indicates that adsorption of dyes on to PSP is controlled by exothermic process, and the maximum adsorption is nearly 98.25% and 95.51% for 120 min at 70°C for MB and Rh-6G respectively and the removal of dye is 24.5616 mg/g and 24.8663 mg/g for MB and Rh-6G respectively.

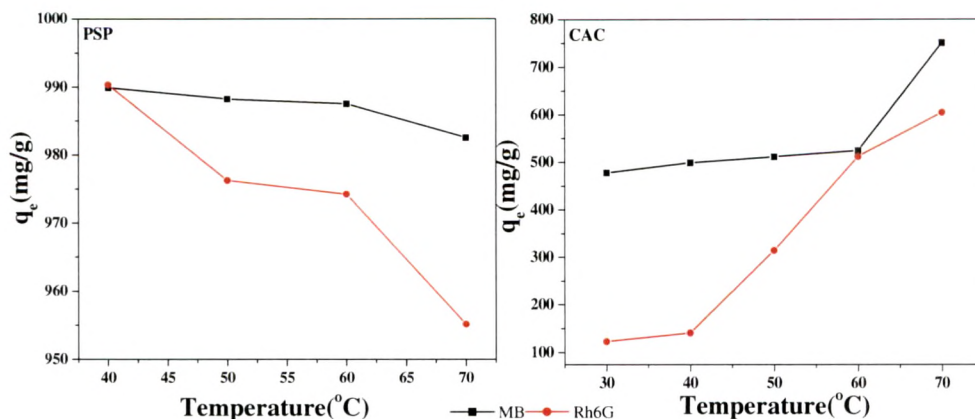


Figure 2.8: Variation in the temperature of dyes on PSP and CAC

Table 2.8: Effect of Temperature on MB and Rh6G removal by PSP

Adsorbent: PSP, adsorbate: Rhodamine 6G, Methylene blue; Temperature: 40-70 °C, Initial concentration: 100ppm, Wt. of adsorbent: 0.1 g; Volume of aqueous phase: 25mL, Contact time: 120 min, pH: 6.54(MB), 5.75(Rh6G)

Time (min)	Percentage uptake of anionic dyes							
	(40°C)		(50°C)		(60°C)		(70°C)	
	M.B	Rh 6G	M.B	Rh 6G	M.B	Rh 6G	M.B	Rh 6G
10	98.40	94.06	97.64	92.50	96.08	88.09	94.64	83.98
20	98.51	94.38	97.85	93.67	97.54	89.77	96.68	88.59
30	98.60	96.36	98.49	95.08	98.40	91.99	96.76	88.87
60	98.84	97.59	98.71	96.02	98.60	94.14	97.76	92.11
120	98.99	99.03	98.82	97.62	98.75	97.42	98.25	95.51

**Table 2.9: Effect of Temperature on MB & Rh6G removal by CAC**

Adsorbent: CAC; adsorbate: Rhodamine 6G, Methylene blue; Temperature: 30-70°C, Initial concentration: 100ppm, Wt. of adsorbent: 0.2 g; Volume of aqueous phase: 25mL, Contact time: 120 min, pH: 6.54(MB), 5.75(Rh6G)

Time (min)	Percentage uptake of anionic dyes									
	(30°C)		(40°C)		(50°C)		(60°C)		(70°C)	
	M.B	Rh 6G	M.B	Rh 6G	M.B	Rh 6G	M.B	Rh 6G	MB	Rh6G
10	27.71	-	28.64	-	30.97	2.80	32.46	6.15	47.29	9.50
20	30.04	0.83	30.97	1.81	39.13	4.97	45.20	8.71	49.58	16.99
30	31.44	2.21	32.37	3.39	40.30	11.67	48.46	13.84	53.13	27.05
60	34.24	7.93	38.43	11.67	41.70	13.84	54.52	24.68	62.92	55.64
120	47.76	12.26	49.86	14.04	51.12	31.39	52.43	51.10	75.05	60.37

In the case of CAC % removal increased as the temperature increases with increase in time and the maximum adsorption is nearly 75% and 60% at 120 min at 70°C for MB and Rh-6G respectively and the removal of dye is 18.76 mg/g and 15.09 mg/g for MB and Rh-6G respectively. Results show that temperature plays an important role on the dye adsorption capacity of PSP. At high temperature, the thickness of the boundary layer decreases, due to the increased tendency of the dye to escape from the biomass surface to the solution phase, which results in a decrease in adsorption as temperature increases [2.9].

The decrease in adsorption with increasing temperature, suggests weak adsorption interaction between biomass surface and the dye, which supports physisorption where as in the case of CAC it is chemisorption.

### 2.6.5 Thermodynamic studies:

Thermodynamic parameters such as  $\Delta G^0$ ,  $\Delta H^0$  and  $\Delta S^0$  were determined using standard thermodynamic relationships.

The free energy of adsorption,  $\Delta G^0$ , can be related to the equilibrium constant  $K_a$  ( $L \cdot mol^{-1}$ ), corresponding to the reciprocal of the Langmuir constant  $K_a$  [2.10]

$$\Delta G^0 = -RT \ln K_a \quad (1)$$

where R is the gas universal constant ( $8.314 J \cdot mol^{-1} \cdot K^{-1}$ ) and T is the absolute temperature.

The changes in enthalpy,  $\Delta H^0$ , and entropy,  $\Delta S^0$ , can be estimated by

$$\ln K_a = \Delta S^0/R - \Delta H^0/(RT) \quad (2)$$

From Table 2.10 it is evident that the negative values of apparent enthalpy change show an exothermic physical adsorption favoured by decreased temperature. The negative values of  $\Delta G^0$  confirm that the basic dye adsorption on PSP is a spontaneous process. It has been reported that  $\Delta G^0$  up to  $-20$  kJ/mol are due to electrostatic interaction between adsorption sites and the adsorbate (physical adsorption), while  $\Delta G^0$  values more negative than  $-40$  kJ/mol involve charge sharing or charge transfer from the adsorbent surface to the adsorbate to form a coordinate bond (chemical adsorption)[2.11]. The  $\Delta G^0$  values obtained in this study for the two dyes are  $<-10$  kJ/mol, which indicates that physical adsorption was the predominant mechanism in the adsorption process.

The apparent entropy change values are almost constant over the temperature range. The positive entropy characterize an increased disorder of the system due to the loss of water which surrounding the dye molecules at the adsorption on the PSP. It can be suggested that the driving force for adsorption process is an entropy effect [2.12].

**Table 2.10: Thermodynamic Parameters for Rhodamine 6G and Methylene Blue at different time and temperature intervals**

Adsorbent: PSP; adsorbate: Rhodamine 6G, Methylene blue; Temperature: 30°C, Initial concentration: 100ppm, Wt. of adsorbent: 0.1g; Volume of aqueous phase: 25mL, Contact time: (10-120) min, pH: 6.54(MB), 5.75(Rh6G)

Time (min)	Temp. (K)	Rhodamine6G				Methylene Blue			
		ln K <sub>a</sub>	-ΔG <sup>0</sup> KJ/mol	ΔS <sup>0</sup> KJ/mol	-ΔH <sup>0</sup> KJ/mol	Ln K <sub>a</sub>	-ΔG <sup>0</sup> KJ/mol	ΔS <sup>0</sup> KJ/mol	-ΔH <sup>0</sup> KJ/mol
120	313	3.2314	8.4090	-	-	3.2013	8.6607	-	-
	323	2.3168	6.2217	0.2573	76.8728	3.0455	8.1784	0.0659	13.0996
	333	2.2360	6.1906	0.1481	43.1270	2.9832	8.2590	0.0532	9.4526
60	313	2.3035	5.9943	-	-	3.0617	7.9673	-	-
	323	1.7860	4.7962	0.1493	43.4256	2.9534	7.9310	0.0527	9.1025
	333	1.3804	3.8218	0.1316	39.9931	2.8688	7.9426	0.0489	8.3540
30	313	1.8799	4.8919	-	-	2.8688	7.4655	-	-
	323	1.5648	4.2022	0.0971	26.4814	2.7907	7.4943	0.0435	6.5644
	333	1.0447	2.8924	0.1173	36.1838	2.7299	7.5579	0.0408	6.0201
20	313	1.4238	3.7051	-	-	2.8034	7.2951	-	-
	323	1.2984	3.4869	0.0434	10.5351	2.4338	6.5358	0.1164	31.0626
	333	0.7747	2.1447	0.0856	26.3715	2.2927	6.3474	0.0855	22.1264
10	313	1.3664	3.5557	-	-	2.7358	7.1194	-	-
	323	1.1158	2.9965	0.0745	21.0586	2.3365	6.2739	0.1234	33.5820
	333	0.6036	1.6711	0.1044	33.0489	1.8134	5.0204	0.1351	39.9691

### 2.6.6 Column studies:

Column studies were conducted using down flow technique, 1.0 g of PSP was transferred into glass column of 1cm diameter. The column height is about 3 cm. Glass wool was kept at the bottom of the column to avoid the loss of adsorbent with the liquid flow. The dye solution was fed into the column at a flow rate of 1mL/min and definite volumes of the effluent were collected. The initial amount of the dye in

the fraction passed and the amount found in the effluent fraction gave the amount of dye retained by the adsorbent. The pH of the solution was maintained at its original pH- 6.54 for Methylene Blue and 5.75 for Rhodamine 6G.

The break through capacity of MB and Rh6G when a column is used was studied by passing 100 ppm solution of both the dyes. The ratio  $C_e/C_o$  where  $C_e$  is the initial concentration of dye in the effluent and  $C_o$  is the dye in the feed was calculated. A graph was plotted of  $C_e/C_o$  versus volume of solution passed as shown in Figure 2.9. From Figure 2.9 it is evident that the volumes of aqueous solution containing 100 ppm of dye that can be treated are 1.215 L and 1.005 L for MB & Rh6G respectively. The exhaustive capacities determined are 121.5 and 105.0 mg/g for MB and Rh6G respectively.

The PSP was used for the removal of Rh6G from an effluent coming from Rh6G manufacturing industry. 300 mL of effluent containing 150 ppm of Rh6G could be treated. The exhaustive capacity determined was 45 mg/g. In the packed column, the available active sites of adsorbent are minimum. So, the amount of dye adsorbed was found to be less when compared with batch adsorption experiments.

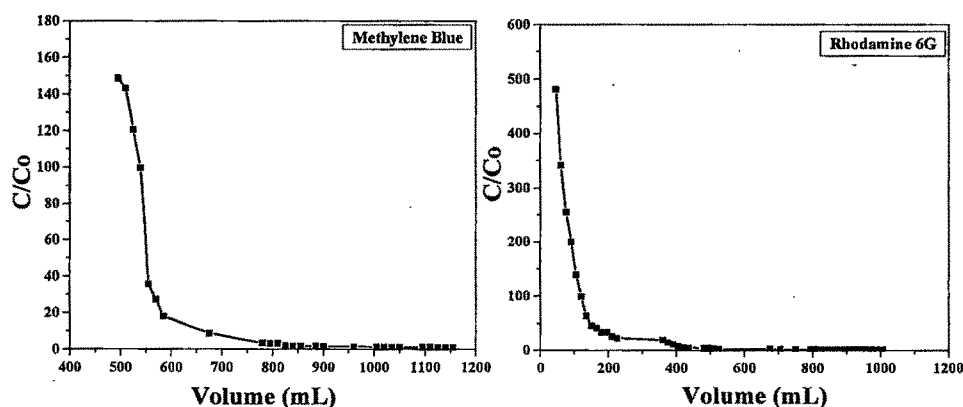


Figure 2.9: Break through graphs of MB & Rh6G

### 2.6.7 Adsorption Isotherms:

Proper analysis and design of adsorption separation processes requires relevant adsorption equilibria as one of the vital information. In equilibrium, a certain relationship prevails between solute concentration in solution and adsorbed state (i.e., the amount of solute adsorbed per unit mass of adsorbent). Their equilibrium concentrations are a function of temperature. Therefore, the adsorption equilibrium relationship at a given temperature is referred to as adsorption isotherm. Several adsorption isotherms originally used for gas phase adsorption are available and readily adopted to correlate adsorption equilibria in adsorption. The most widely used among them are Freundlich and Langmuir equations. The application of these isotherms is discussed. The results of the adsorption experiments were analyzed using Freundlich, Langmuir models to determine the mechanistic parameters associated with adsorption.

#### 2.6.7a Freundlich isotherm:

Freundlich isotherm is an empirical equation. This equation is one among the most widely used isotherms for the description of adsorption equilibrium. Freundlich isotherm is capable of describing the adsorption of organic and inorganic compounds on a wide variety of adsorbents including biosorbent. This equation has the following form

$$q_e = K_f C_e^{1/n} \quad (3)$$

Eq. (3) can also be expressed in the linearized logarithmic form

$$\text{Log } q_e = \text{log } K_f + 1/n \text{ log } C_e \quad (4)$$

The plot of  $\log q_e$  versus  $\log C_e$  has a slope with the value of  $1/n$  and an intercept magnitude of  $\log K_f$ .  $\log K_f$  is equivalent to  $\log q_e$  when  $C_e$  equals unity. However, in other case when  $1/n = 1$ , the  $K_f$  value depends on the units upon which  $q_e$  and  $C_e$  are expressed. On average, a favorable adsorption tends to have Freundlich constant  $n$  between 1 and 10. Larger value of  $n$  (smaller value of  $1/n$ ) implies stronger interaction between adsorbent and adsorbate while  $1/n$  equal to 1 indicates linear adsorption leading to identical adsorption energies for all sites [2.13]. As a robust equation, Freundlich isotherm has the ability to fit nearly all experimental adsorption–desorption data, and is especially excellent for fitting data from highly heterogeneous adsorbent systems.

#### **2.6.7b Langmuir isotherm:**

Another widespread-used model for describing adsorbate sorption is the Langmuir model. Langmuir equation relates the coverage of molecules on a solid surface to concentration of a medium above the solid surface at a fixed temperature. This isotherm is based on three assumptions, namely adsorption is limited to monolayer coverage, all surface sites are alike and only can accommodate one adsorbed atom and the ability of a molecule to be adsorbed on a given site is independent of its neighbouring sites occupancy. By applying these assumptions, and a kinetic principle (rate of adsorption and desorption from the surface is equal), the Langmuir equation can be written in the following form

$$q_e = q_{\max} (K_a C_e / (1 + K_a C_e)) \quad (5)$$

This equation is often written in different linear forms [2.21, 2.29]

$$C_e / q_e = (1/q_{\max}) C_e + 1/(K_a q_{\max}) \quad (6)$$

$$1/q_e = (1/K_a q_{\max})1/C_e + (1/q_{\max}) \quad (7)$$

$$q_e = q_{\max} - (1/K_a)(q_e/C_e) \quad (8)$$

$$(q_e/C_e) = K_a q_{\max} - K_a q_e \quad (9)$$

The decrease of  $K_a$  value with temperature rise signifies the exothermicity of the adsorption process (physical adsorption) [2.15, 2.26-2.29], while the opposite trend indicates that the process needs thermal energy (endothermic), leading to chemisorptions [2.14, 2.16-2.25]. In physical adsorption, the bonding between adsorbate and active sites of the adsorbent weakens at higher temperature in contrast with chemisorptions bonding which becomes stronger.

The data obtained from the isotherm studies were tested for applicability to the above two isotherm models (Figure 2.10). Tables 2.11 show the values of the parameters of the two isotherms and the related correlation coefficients.

From Table 2.11 it can be observed that MB conforms to the Freundlich isotherm model for adsorption onto PSP. The values of  $1/n$ , less than unity for MB is an indication that significant adsorption takes place at low concentration but the increase in the amount adsorbed with concentration becomes less significant at higher concentration and vice versa[2.30].

**Table 2.11: Isotherm Constants**

Adsorbent: PSP; adsorbate: Rhodamine 6G, Methylene blue; Temperature: 30°C, Initial concentration: 100ppm, Wt. of adsorbent: (0.05-0.4) g; Volume of aqueous phase: 25mL, Contact time: (10-120) min, pH: 6.54(MB), 5.75(Rh6G)

Isotherm	Parameter	MB	Rh6G
Freundlich	$K_f(\text{mg/g})(\text{dm}^3/\text{mg})^{1/n}$	0.6605	-2.4654
	N	1.2681	1.9786
	$r^2$	0.9449	0.9250
	1/n	0.7886	1.9786
Langmuir	$q_c(\text{mg/g})$	12.3781	11.9956
	$q_m(\text{mg/g})$	4.2512	19.6531
	$K_a(\text{L/mg})$	0.0399	-0.1035
	$r^2$	0.9423	0.9813

Negative values for the Langmuir isotherm constant indicate the inadequacy of this model to explain the adsorption process, since the constant represents the surface binding energy. For MB however, adsorption onto PSP conforms to both the Langmuir and Freundlich models. From the Figure 2.10 it is evident that, the linear plots of Freundlich and Langmuir models were good fit in the case of Methylene blue but in the case of Rhodamine 6G Freundlich is some what better than Langmuir model. Table 2.12 shows the comparison of maximum monolayer adsorption capacity of some cationic dyes on various adsorbents reported in the literature along with PSP used in this work

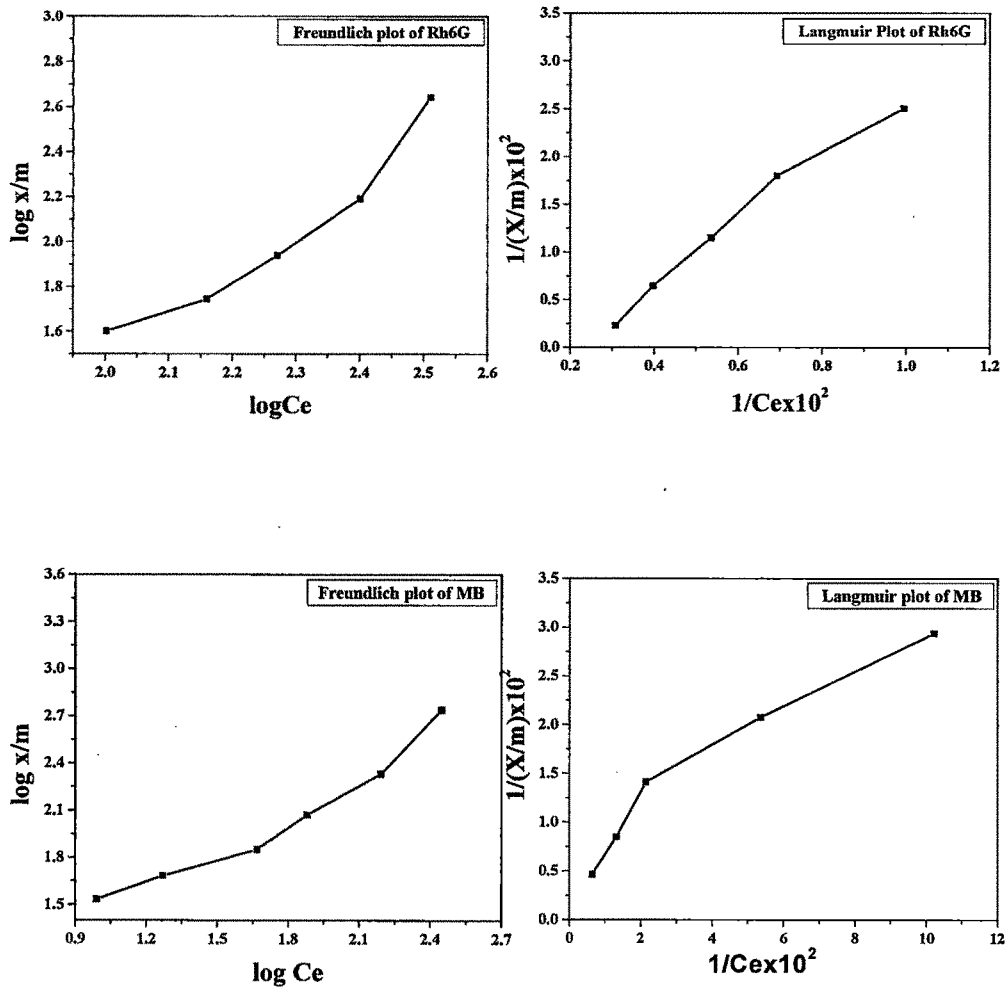


Figure: 2.10: Freundlich and Langmuir adsorption isotherm plots of MB & Rh6G

**Table 2.12: Comparison of adsorption capacities of cationic dyes on other adsorbents**

Material	Dye	mg/g	References
Pyrolyzed petrified sediment	Methylene Blue	2.39	[2.39]
Carbon from scrap tires	Rhodamine B	307.2	[2.40]
Grape fruit peel	Crystal violet	254	[2.41]
Fuel oil fly ash	Methylene blue	47	[2.42]
Peat	Methylene blue	190-240	[2.43]
Bentonite	Methylene Blue	48.309	[2.44]
Activated carbon- epicarp of Ricinus communis	malachite green	99.04%	[2.45]
Carbon- Arundo donax root	malachite green	8.69	[2.46]
Activated carbon- Euphorbia rigida (H <sub>2</sub> SO <sub>4</sub> activation)	methylene blue	114.45	[2.47]
Apricot stone activated carbon	Basic dye	221.23	[2.48]
PSP	MB	4.2512	Present study
PSP	Rh6G	19.6531	Present study

### 2.6.8 Adsorption Dynamics:

Adsorption equilibria studies are important to determine the efficacy of adsorption. In spite of this, it is also necessary to identify the adsorption mechanism type in a given system. For the purpose of investigating the mechanism of adsorption and its potential rate-controlling steps that include mass transport and chemical reaction processes, kinetic models have been exploited to test the experimental data. In addition, information on the kinetics of adsorbate uptake is required to select the optimum condition for full-scale batch removal processes. Adsorption kinetics is expressed as the solute removal rate that controls the residence time of the adsorbate

in the solid–solution interface. In practice, kinetic studies are carried out in batch reactions using various initial adsorbate concentrations, adsorbent doses, particle sizes, agitation speeds, pH values and temperatures along with different adsorbent and adsorbate types. Then, linear regression is used to determine the best-fitting kinetic rate equation. [2.31]

Several adsorption kinetic models have been established to understand the adsorption kinetics and rate-limiting step. These include pseudo-first and pseudo-second-order rate model, Weber and Morris adsorption kinetic model, The pseudo-first and pseudo-second-order kinetic models are the most well studied models.

#### 2.6.8a The pseudo-first-order kinetic:

The Lagergren first-order rate expression based on solid capacity is generally expressed as follows

$$dq/dt = K_1(q_e - q) \quad (10)$$

Integration of Eq. (10) with the boundary conditions as follow:  $t=0$ ,

$q = 0$ , and at  $t = t$ ,  $q = q$ , gives

$$\ln(q_e - q) = \ln q_e - K_1 t \quad (11)$$

Eq. (12) can be written in the non-linear form

$$q = q_e (1 - \exp(-K_1 t)) \quad (12)$$

Hypothetically, to ascertain the rate constants and equilibrium metal uptake, the straight-line plots of  $\log(q_e - q)$  against  $t$  of Eq.(11) were made at different initial adsorbate concentrations[2.32]. The  $q_e$  value acquired by this method is then contrasted with the experimental value. If large discrepancies are posed, the reaction

cannot be classified as first-order although this plot has high correlation coefficient from the fitting process.

In order to obtain the rate constants, the straight-line plots of  $\log (q_e - q)$  against  $t$  were made for PSP at different initial dye concentrations (Figure 2.11). The intercept of the above plot should be equal to  $\log q_e$ . However, if the intercept is not equal to the equilibrium dye uptake then the reaction is not likely to be first order even if this plot has high correlation coefficient with the experimental data [2.36]. Correlation coefficients were found to be between 0.9874 and 0.9723 for MB and Rh6G respectively but the calculated  $q_e$  was found to be not equal to experimental  $q_e$ , suggesting the insufficiency of Pseudo-first order model to fit the kinetic data for the initial dye concentrations examined. A time lag, probably caused by the presence of boundary layer or external resistance controlling at the beginning of the adsorption process was argued to be the responsible factor behind the discrepancy [2.33]. The negative values of the rate constant suggest that pseudo first order is not a good fit. The rate constants and the correlation coefficients for all concentrations tested have been summarized in Table 2.13

#### **2.6.8b The pseudo-second-order kinetic:**

Predicting the rate of adsorption for a given system is among the most important factors in adsorption system design, as the system's kinetics determines adsorbate residence time and the reactor dimensions [2.34]. As previously noted that although various factors govern the adsorption capacity, i.e., initial adsorbate concentration, temperature, pH of solution, adsorbent particle size, adsorbate nature, a kinetic model is only concerned with the effect of observable parameters on the overall rate [2.31].

Pseudo-second order model is derived on the basis of the adsorption capacity of the solid phase, expressed as

$$dq/dt = K_2(q_e - q)^2 \quad (13)$$

Integration of Eq. (14) with the boundary conditions  $t=0, q = 0$ , and at  $t = t, q = q$ , results in

$$1/(q_e - q) = 1/q_e + K_2 t \quad (14)$$

Eq. (15) can be stated in the linear form as

$$t/q = t/q_e + 1/K_2 q_e^2 \quad (15)$$

The pseudo-second-order rate constants were determined experimentally by plotting  $t/q$  against  $t$ .

A straight line could be obtained and  $q_e$  and  $K_2$  could be calculated. Good fits were observed for all initial concentrations (Figure 2.11) indicating that adsorption reaction can be approximated with the Pseudo-second-order model.

Correlation coefficients are tabulated along with the rate constants in Table 2.13 which were found to be 1.000 and 0.9999 for MB and Rh6G respectively, and the calculated  $q_e$  values obtained from the second-order kinetic model agree with the experimental  $q_e$  values for both the cases.

These suggest that the adsorption of dyes onto PSP follows the second-order kinetic model and chemical adsorption might be the rate-limiting step. Since PSP in our experiments has very high equilibrium adsorption capacity  $q_e$ , the adsorption rates are very fast and the equilibrium times short. The adsorption capacities  $q_t$  of the dyes at 10 min for almost all the initial concentrations reached over 98% of the calculated equilibrium adsorption capacities. Such short equilibrium times coupled with high adsorption capacity indicate a high degree of affinity between the dyes and PSP [2.37]

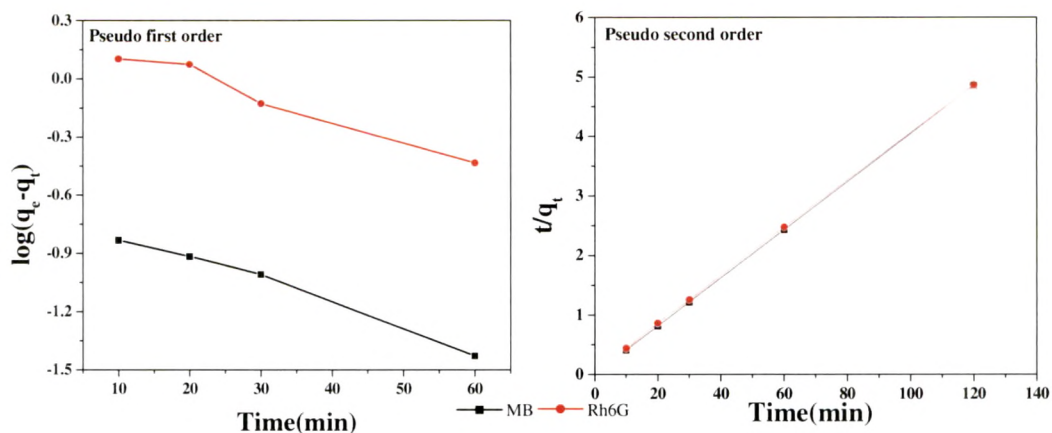


**Figure 2.11: Pseudo First-order and Pseudo Second-order graphs of MB & Rh6G**

**Table 2.13: Kinetic parameters for cationic dyes**

Adsorbent: PSP; adsorbate: Rhodamine 6G, Methylene blue; Temperature: 30°C, Initial concentration: 100ppm, Wt. of adsorbent: 0.2 g; Volume of aqueous phase: 25mL, Contact time: (10-120) min, pH: 6.54(MB), 5.75(Rh6G)

Kinetics	Parameter	MB	Rh6G
Experimental	$q_e$ (mg/g)	24.7481	24.7555
Pseudo-First Order	$q_e$ (mg/g)	18.858	23.1096
	$K_1$ ( $\text{min}^{-1}$ )	-0.0122	-0.0113
	$r^2$	0.9874	0.9723
Pseudo-Second Order	$q_e$ (mg/g)	24.7525	24.9377
	$K_2$ (g/mgmin)	0.0046	0.04013
	$r^2$	1.0000	0.9999
Intra-particle	$K_i$ ( $\text{mg/gmin}^{0.5}$ )	0.05724	0.0237
	$r^2$	0.9356	0.9699

### 2.6.8c Intraparticle Diffusion:

According to the model of intra-particles diffusion based on the theory proposed by Weber and Morris [2.35] a graphic plot for adsorption capacity at time  $t$ ,  $q_t$ , versus square root of time,  $t^{0.5}$ , should be linear for a rate controlled by intra-particle-diffusion.

The linear form of the equation:

$$q_t = K t^{0.5} \quad (16)$$

indicates that, if the intra-particles diffusion is the sole rate controlling step, the plot should be linear through the origin.

Study of intra-particle diffusion model gave  $r^2$  values of 0.9699 for Rh6G and 0.9356 for MB and plot between adsorbate concentration and square root of time was linear suggesting that adsorption process could be controlled by intra-particle diffusion.

### 2.6.9 Banghams equation:

The Bangham equation indicates a direct proportionality between the length change of a porous body and a change of surface energy.

Bangham's equation is employed to further confirm whether the adsorption process is diffusion controlled. [2.38]

$$\log \log [C_0 / (C_0 - q' m')] = \log (K_0 m' / 2.303V) + \alpha \log t \quad (17)$$

where  $C_0$  is initial concentration of adsorbate in solution (mmol/L),  $V$  is volume of solution (mL),  $m'$  is weight of adsorbent used per liter of solution (g/L),  $q'$  is the amount of adsorbate retained at time  $t$  (mmol/g),  $\alpha$  and  $K_0$  are constants. The double logarithmic plot according to equation (17) yielded linear curves showing that the

diffusion of the adsorbate into the pores of the adsorbent perfectly controls the adsorption process. The plots obtained for  $\log\log [C_0/C_0 - q/m]$  against  $\log t$  (Figure 2.12) were linear with good correlation coefficients (MB: 0.9789, Rh6G: 0.9499). The results thus conform to Bangham's equation and indicate that the adsorption of the dye is pore diffusion controlled process.

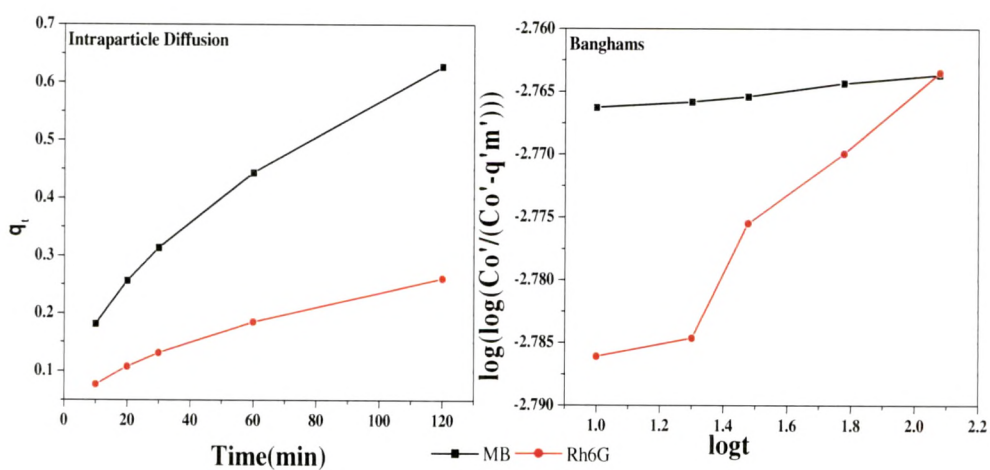


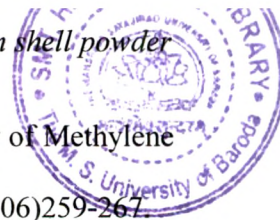
Figure 2.12: Intra-particle diffusion and Banghams plots of Cationic dyes

## **2.7 Conclusions:**

Palm Shell Powder is a promising adsorbent for removal of the cationic dyes, Methylene Blue and Rhodamine 6G from water. The surface of the PSP particles was heterogeneous, non-specific and non-uniform in nature. Different operational parameters observed during the process of investigations reveal that the pH, temperature, contact time, adsorbent dose and concentrations of the adsorbate govern the overall process of adsorption. The batch studies clearly demonstrate that there is > 94 % removal for concentrations as high as 500 ppm. The exhaustive capacities determined are 121.5 and 105.0 mg/g of adsorbent for MB and Rh6G respectively. The equilibrium adsorption is achieved in 120 min. The adsorption of Methylene Blue on PSP was exothermic. However Pseudo second order model is the best fit for the adsorption of dyes onto PSP suggesting that the adsorption of dyes by PSP may involve not only physisorption but also chemisorption. PSP was found to be more effective than CAC for the removal of MB and Rh6G. In addition it is a low cost adsorbent. PSP was found to be effective for the removal of Rh6G from effluent.

**References:**

- 2.1. Mishra, G. and Tripathy, M., "A critical review of the treatment for decolorization of dye wastewater", *Colourage*, 40 (1993) 35–38.
- 2.2. Hunger K., "Industrial Dyes: Chemistry, Properties, Applications," Wiley-VCH, Weinheim, (2003).
- 2.3. Vasanth Kumar K, Ramamurthi V, and Sivanesan S, "Modelling the mechanism involved during the sorption of methylene blue onto fly ash," *Journal of colloid interface science*, 284 (2005) 14-21.
- 2.4. M. Rafatullah, O. Sulaiman, R. Hashim, A. Ahmad, "Adsorption of Methylene Blue on low cost adsorbents: A review," *J. Hazard. Mater.*, 177 (2010) 70.
- 2.5. Suzuki, R.M., Andrade, A.D., Sousa, J.C. and Rollemberg, M.C., "Preparation and Characterisation of Activated Carbon from rice bran", *Bioresource Technology*, 98(2007), 1985-1991.
- 2.6. Naizhen, C., Darmstadt, H. and Christian, R., "Activated Carbon produced from charcoal obtained by vacuum pyrolysis of softwood bark residues," *Energy and Fuels*, 15(2001) 1263-1269.
- 2.7. Rao K.C.L.N., Krishnaih K. and Ashutosh, "Colour removal from a Dyestuff Industry Effluent Using Activated Carbon", *Indian J Chem. Tech.*, 1 (1994) 13.
- 2.8. Aharoni, C. and Ungarish, M., "Kinetics of activated chemisorption. Part II. Theoretical models", *J.Chem.Soc. Faraday Trans.*, 73 (1977) 456.
- 2.9. Tutem E, Apak R and Unal CF, "Adsorptive removal of chlorophenols from water by bituminous coal," *Water Res.*, 32(8) (1998)2315.



- 2.10. Bulut, Y., Aydin, H., “A kinetics and thermodynamics study of Methylene blue adsorption on wheat shells”, *Desalination*, 194 (1-3) (2006)259-267.
- 2.11. Horsfall M, Spiff AI, Abia AA, “Studies on the influence of mercaptoacetic acid (MAA) modification of cassava (*Manihot sculsculenta* cranz) waste Biomass on the adsorption of  $\text{Cu}^{2+}$  and  $\text{Cd}^{2+}$  from aqueous solution”, *Bull. Korean Chem. Soc.*, 25 (7) (2004) 969-976.
- 2.12. Raghuvanshi SP, A.K.Raghav, R.Singh and A.Chandra, “Investigation of sawdust as Adsorbent for the removal of Methylene Blue Dye in aqueous Solution. Proceedings of International conference for water and waste water perspectives in developing countries (NAPDEC)”, *International water association, U.K.*, (99)(2002)1053-1062.
- 2.13. Delle Site, A., “Factors affecting sorption of organic compounds in natural sorbent/ water systems and sorption coefficients for selected pollutants. A review”, *Journal of Physical and Chemical Reference Data*, 30 (2001) 187–439.
- 2.14. Dursun, A.Y., “A comparative study on determination of the equilibrium, kinetic and thermodynamic parameters of biosorption of copper (II) and lead (II) ions onto pretreated *Aspergillus niger*,” *Biochemical Engineering Journal*, 28 (2006)187–195.
- 2.15. Ho, Y. and Ofomaja, A.E., “Biosorption thermodynamics of cadmium on coconut copra meal as biosorbent”, *Biochemical Engineering Journal*, 30 (2006) 117–123.
- 2.16. Malkoc, E. and Nuhoglu, Y., “Investigations of nickel (II) removal from aqueous solutions using tea factory waste”, *Journal of Hazardous Materials*, B127 (2005) 120–128.

- 2.17. Wang, X., Qin, Y., and Li, Z., "Biosorption of zinc from aqueous solutions by rice bran: kinetics and equilibrium studies", *Separation Science and Technology*, 41 (2006) 747–756.
- 2.18. Deng, L., Su, Y., Su, H., Wang, X. and Zhu, X., "Biosorption of copper (II) and lead (II) from aqueous solutions by nonliving green algae *Cladophora fascicularis*: equilibrium, kinetics and environmental effects", *Adsorption*, 12 (2006) 267–277.
- 2.19. Antunes, W.M., Luna, A.S., Henriques, C.A. and Costa, A.C.A., "An evaluation of copper biosorption by a brown seaweed under optimized conditions", *Electronic Journal of Biotechnology*, 6 (2003) 174–184.
- 2.20. Dundar, M., Nuhoglu, C. and Nuhoglu, Y., "Biosorption of Cu(II) ions onto the litter of natural trembling poplar forest", *Journal of Hazardous Materials*, 151 (2008) 86–95.
- 2.21. Aydin, H., Bulut, Y. and Yerlikaya, C., "Removal of copper (II) from aqueous solution by adsorption onto low-cost adsorbents", *Journal of Environmental Management*, 87 (2008) 37–45.
- 2.22. Gupta, V.K. and Rastogi, A., "Biosorption of lead from aqueous solutions by green algae *Spirogyra* species: kinetics and equilibrium studies", *Journal of Hazardous Material*, 152 (2008) 407–414.
- 2.23. Ho, Y., "Isotherms for the sorption of lead onto peat: comparison of linear and non-linear methods", *Polish Journal of Environmental Studies*, 15 (2006) 81–86.
- 2.24. Green-Ruiz, C., Rodriguez-Tirado, V. and Gomez-Gil, B., "Cadmium and zinc removal from aqueous solutions by *Bacillus jeotgali*: pH, salinity and temperature effects", *Bioresource Technology*, 99 (2008) 3864–3870.

- 2.25. Vilar, V.J.P., Botelho, C.M.S. and Boaventura, R.A.R. "Copper removal by algae *Gelidium*, agar extraction algal waste and granulated algal waste: kinetics and equilibrium", *Bioresource Technology*, 99 (2008) 750–762.
- 2.26. Padmavathy, V., "Biosorption of nickel (II) ions by baker's yeast: kinetic, thermodynamic and desorption studies", *Bioresource Technology* 99 (2008) 3100–3109.
- 2.27. Djeribi, R., and Hamdaoui, O., "Sorption of copper (II) from aqueous solutions by cedar sawdust and crushed brick", *Desalination*, 225 (2008) 95–112.
- 2.28. Jnr, M.H. and Spiff, A.I., "Effects of temperature on the sorption of  $Pb^{2+}$  and  $Cd^{2+}$  from aqueous solution by *Caladium bicolour* (Wild Cocoyam) biomass", *Electronic Journal of Biotechnology*, 8 (2005) 162–169.
- 2.29. Shaker, M.A., "Thermodynamic profile of some heavy metal ions adsorption onto biomaterial surfaces", *American Journal of Applied Sciences*, 4 (2007) 605–612.
- 2.30. Hsisheng, T. and Chien-To, H., "Influence of Surface Characteristics on Liquid-Phase Adsorption of Phenol by Activated Carbons Prepared from Bituminous Coal," *Ind. Eng. Chem. Res.*, 39(9) (1998) 3618-3624.
- 2.31. Ho, Y., "Second-order kinetic model for the sorption of cadmium onto tree fern: a comparison of linear and non-linear methods", *Water Research*, 40 (2006) 119–125.
- 2.32. Ho, Y.S. and McKay, G., "Application of kinetic models to the sorption of copper (II) on to peat", *Adsorption Sciences & Technology*, 20 (2002) 797–815.

*Chapter 2: Adsorption of Cationic dyes with Palm shell powder*

- 2.33. Vijayaraghavan, K., Palanivelu, K. and Velan, M., “Biosorption of copper (II) and cobalt (II) from aqueous solutions by crab shell particles”, *Bioresource Technology*, 97 (2006) 1411–1419.
- 2.34. Ho, Y., “Review of second-order models for adsorption systems”, *Journal of Hazardous Materials*, B136 (2006) 681–689.
- 2.35. Weber, J.R. and Morris, J.C. “Kinetics of adsorption on carbon from solutions”, *J. Sanit. Eng. Div. Am. Soc. Civ. Engrs.*, 89 (1963) 31.
- 2.36. Ho, Y.S. and, McKay, G., “Sorption of dye from aqueous solution by peat”, *Chemical Engineering Journal*, 70(2) (1998) 115-124.
- 2.37. Aksu, Z., “Biosorption of Reactive Dyes by Dried Activated Sludge: Equilibrium and Kinetic Modeling”, *Biochem.Eng. J.*, 7 (2001) 79.
- 2.38. Ola. A., “Kinetic and Isotherm studies of Copper (II) removal from wastewater using various Adsorbents”, *Egyptian Journal of Aquatic Research*, 33(1) (2007) 125-143.
- 2.39. Ayse Z. Aroguz, J. Gulen, R.H. Evers, “Adsorption of methylene blue from aqueous solution on pyrolyzed petrified sediment”, *Bioresource Technology*, 99 (2008) 1503–1508.
- 2.40. Li, Li., Liu, S. and Zhu, T., “Application of activated carbon derived from scrap tires for adsorption of Rhodamine B”, *Journal of Environmental Sciences*, 22(8) (2010) 1273–1280.
- 2.41. Saeed, A., Sharif, M. and Iqbal, M., “Application potential of grapefruit peel as dye sorbent: Kinetics, equilibrium and mechanism of crystal violet adsorption”, *Journal of Hazardous Materials*, 179 (2010) 564–572.

- 2.42. Andini, S., Cioffi, R., Colangelo, F., Montagnaro, F. and Santoro, L., "Adsorption of chlorophenol, chloroaniline and methylene blue on fuel oil fly ash", *Journal of Hazardous Materials*, 157 (2008) 599–604.
- 2.43. Andreia, N.F., Carlos A., Policiano, A, Nito, A.D. and Maria, M., "Isotherm and thermodynamic data of adsorption of methylene blue from aqueous solution onto peat", *Journal of Molecular Structure*, 982(1-3) (2010) 62-65.
- 2.44. Ceyda, B., "Investigation of the factors affecting organic cation adsorption on some silicate minerals," *Journal of Colloid and Interface Science*, 281 (2005) 33–38.
- 2.45. T. Santhi, T., Manonmani, S. and Smitha, T., "Removal of malachite green from aqueous solution by activated carbon prepared from the epicarp of *Ricinus communis* by adsorption", *Journal of Hazardous Materials*, 179 (2010) 178–186.
- 2.46. Zhang, J., Li, Y., Zhang, C. and Jing, Y., "Adsorption of malachite green from aqueous solution onto carbon prepared from *Arundo donax* root," *Journal of Hazardous Materials*, 150 (2008) 774–782.
- 2.47. Ozgu"l, G., Adnan, O., Safa, A.O., and Gerc, H.F., "Preparation of activated carbon from a renewable bio-plant of *Euphorbia rigida* by H<sub>2</sub>SO<sub>4</sub> activation and its adsorption behavior in aqueous solutions", *Applied Surface Science*, 253 (2007) 4843–4852.
- 2.48. Demirbas, E., Kobya, M. and Sulak, M.T. "Adsorption kinetics of a basic dye from aqueous solutions onto apricot stone activated carbon", *Bioresource Technology*; 99 (2008) 5368–5373.